Effect of the shape and duration of excitation pulse on the dynamics of excitons and trions in quantum wells

P. Aceituno* and A. Hernández-Cabrera
Departamento Física Básica, Universidad de La Laguna, La Laguna, 38206-Tenerife, Spain
(Received 15 May 2008; revised manuscript received 11 August 2008; published 9 September 2008)

We have studied the effect of the shape and duration of a photoexcitation pulse on the temporal evolution of excited electrons when they are both free or bounded in excitons and trions. A quantum well with *n*- and *p*-type remotely doped regions is considered to get the necessary excess of free electrons or holes. This configuration allows us to study the evolution of both negative and positively charged excitons simultaneously. Calculations have been done using the matrix density formalism to introduce different pulse types. The temporal behavior of the photoluminescence intensity, which is associated with plasma, exciton, and trion, is obtained by means of the two-dimensional density evolution of the different species.

DOI: 10.1103/PhysRevB.78.115308 PACS number(s): 73.20.Mf, 73.50.Gr, 73.40.Gk

I. INTRODUCTION

In the physics of the semiconductors, the electronic affinity of a third charge makes that (under certain circumstances) excitons capture this charge to form the so-called trions or charged excitons. These can be negatively or positively charged depending on where they are formed in an environment with an excess of electrons or holes, respectively. Semiconductor quantum wells (QWs) have demonstrated to be the suitable structures to generate these complex particles. The method most widely used to get the charge generation in these structures is the photoexcitation with an ultrashort laser pulse that causes the same concentration of photoexcited electrons and holes and, therefore, the corresponding excitons. Another method involves the injection of electrons and holes by doping two regions close to the structure. Injection offers the advantage of preventing the interaction between the electromagnetic field associated with the excitation and the excited electrons. In this case, the excitons are created by hole-assisted electron resonant tunnel. Another characteristic of these excitons [direct-created excitons (DCEs)] is that they have spatial coherence, with an in-plane momentum $k_{\mathrm{exc}} \sim 0$, and they can irradiate perpendicularly to the QW. Therefore, DCEs are appropriate for the application in vertical planar microcavities.[1] The injection has two additional advantages: (i) the control of electron and hole densities by means of the impurity concentrations, together with the application of an external electric field, and (ii) the prevention of the exciton thermalization. This thermalization is an unavoidable consequence of the nontuned laser excitation.

Since the standard way to generate trions is the ultrafast photoexcitation, a detailed analysis of this process deserves special attention. Let us suppose we are using a mixed technique. Not only do we dope the material to have an excess of charges but we also photoexcite the sample. In principle, for low donor doping, DCEs would not be formed because the Fermi level of the reservoir will be below the first conduction-band level. After applying an electric field, the electronic level will be populated by electron resonant tunneling. If, once applied (the field), we photoexcite the sample, we will obtain excitons (photoexcited excitons together with DCEs) in a first stage. Since they are formed in an environment with an excess of electrons or holes, the negatively or positively charged excitons will appear, respectively.

These bound complexes of three particles have a binding energy, which is large enough to make them observable. The most broadly used experimental technique to investigate trions is the time-resolved photoluminescence (PL).[2–4] Recently, generation and recombination processes of excitons and trions have been analyzed using this technique.[4,5] PL has also been used to investigate two-dimensional electron gas (2DEG) in magnetic fields. The application of high magnetic fields increases the binding energy of the negatively charge excitons and allows the study of such species under study because the field isolates to a certain extend trions from the 2DEG. This largely prevents the free-electron—trion interaction. Also, two different classes of trions (singlet and triplet states) appear due to the spin polarization of the 2DEG caused by the magnetic field (see Ref. 6 and references therein).

In this work we study the influence of the shape and duration of excitation pulses on the temporal evolution of free-electron, exciton, and trion densities in photoexcited QWs with the necessary free electron or hole excess. The process of trion generation can be considered as follows. First, if the Fermi level of the *n*-type material (see Fig. 1) resonates with the electronic level in the QW, electrons tunnel to the QW. These electrons, together with holes diffused into the QW,

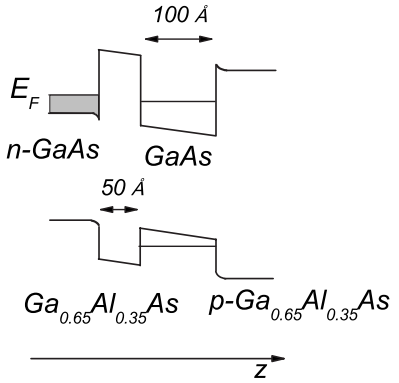

FIG. 1. Scheme of the doped quantum well under study.

form excitons. Second, if there is an excess of electrons or holes, these charges will coexist with DCEs and can give rise to negative or positive trions. Third, if we photoexcite the sample with an ultrashort laser pulse, an additional amount of free electrons and holes are generated and, thus, photoexcited excitons. Some of the excited charges can be bound to excitons leading to the formation of more trions. Thus, we deal with three different electronic states (free, excitonic, and trionic electrons), which will occupy different energy levels. The binding energies for positive (X^+) and negative (X^-) trions in GaAs/AlAs are rather similar according to Teran *et al.*[7] In our case, for a 10 nm QW, they are of the order 1.1 and 0.9 meV, respectively. For a fixed width, these energies depend on the doping concentration due to the built-in electric field but this dependence is weak until concentrations of 10^9 cm^{-2}. Beyond this concentration, the binding energy diminishes for the X^- if the Pauli exclusion principle is considered, leading to the X^- quenching. On the contrary, for positive trions the binding energy slightly increases (initially) with the electric field for small excess concentration of free carriers, and this energy diminishes later because of the exclusion principle. In an actual sample, the excess of concentration of free electrons is of this order of magnitude (10^9 cm^{-2}) or lower. Some authors claim that both species can coexist.[8] We consider this possibility in calculations. Short intense laser pulses can also create neutral biexcitons (XX), which give place to an absorption line some few millielectron volt below the exciton line, close to that of the positive trions. However, Kheng *et al.*[9] and many later works have shown that charged complexes are the most often species in QWs. Thus, we have not considered the biexcitons, which do not contribute essentially to the formation of trions. Coexisting biexciton and trion have rarely been studied.[10]

The aim of this paper is the theoretical analysis of the trion dynamics in the presence of excitons, free electrons, and holes when photoexcited with different laser pulses. We use the matrix density formalism, taking into account the different generation, recombination, and annihilation rates for different types of binding.[11] The effect of the interband optical pulse is included by means of the interband generation function.

II. THEORETICAL FORMALISM

We assume an ultrafast $\delta(t)$ injection of electrons in the QW to simplify calculations when the electronic level lies under the Fermi level. We also suppose a $\delta(t)$ diffusion of holes from the p-doped material to the QW. We consider the excitation laser pulse by means of the function

$$w(t) = \frac{1 + \cosh(\tau_p/2\tau_f)}{[\cosh((t-t_0)/\tau_f) + \cosh(\tau_p/2\tau_f)]}, \tag{1}$$

where τ_p is the pulse duration and $10\tau_f$ is the front pulse duration. Thus, for $\tau_f = 0$ ps we have a square pulse and, for $\tau_f > \tau_p$, the pulse is in a Gaussian-type. Figure 2 shows the shape of the pulse for $\tau_p = 10$ ps and three different τ_f typical values. In order to consider a pulse starting at $t=0$ ps, we have introduced the shift $t_0 = (\tau_p + 10\tau_f)/2$. We first consider the general quantum kinetic equation for the density-matrix

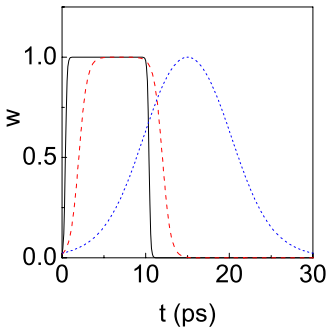

FIG. 2. (Color online) Shape of the pulse for $\tau_p = 10$ ps and $\tau_f = 0.1$ (solid line), 0.5 (dashed), and 2.5 ps (dotted).

operator $\hat{\eta}(t)$ and for electrons placed in an electric field with frequency ω, $\mathbf{E}(t)\exp(-i\omega t) + \text{c.c.} = \mathbf{E}w(t)\exp(-i\omega t) + \text{c.c.}$, and

$$\frac{\partial \hat{\eta}(t)}{\partial t} + \frac{i}{\hbar}[\hat{H}, \hat{\eta}(t)] = \frac{1}{i\hbar}\{[\widehat{\delta H_t} \exp(-i\omega t) + \text{H.c.}], \hat{\eta}(t)\}. \tag{2}$$

Here $\hat{H}$ is the QW one-particle many-band Hamiltonian we have described elsewhere.[11] When electrons are excited by the transverse electric field associated to the laser pulse $E_\perp w(t)\exp(-i\omega t) + \text{c.c.}$, the perturbation operator $\delta\hat{H}_t$, which describes interband transition, can be written as[12]

$$\delta\hat{H}_t = (ie/\omega)E_\perp \hat{v}_\perp w(t), \tag{3}$$

where $\hat{v}_\perp$ is the transverse velocity operator. If we project on the conduction-band states, we find the kinetic equation for the one-electron density matrix $\hat{\rho}(t)$,

$$\frac{\partial \hat{\rho}(t)}{\partial t} + \frac{i}{\hbar}[\hat{H}, \hat{\rho}(t)] = \hat{G}(t) + \hat{J}(\hat{\rho}|t), \tag{4}$$

where $\hat{J}(\hat{\rho}|t)$ is the collision integral and the generation rate is given by

$$\hat{G}(t) = \frac{1}{\hbar^2}\int_{-\infty}^{0} d\tau e^{\lambda\tau - i\omega\tau}[e^{i\hat{H}\tau/\hbar}(\delta\hat{H}_{t+\tau}\hat{\rho}_{eq})e^{i\hat{H}\tau/\hbar}, \delta\hat{H}_t^+] + \text{H.c.}, \tag{5}$$

with the phenomenological constant $\lambda \to +0$. This constant is the finite relaxation rate. Here $\hat{\rho}_{eq}$ is the equilibrium density matrix when the second-order contributions to the response are taken into account.

Taking the basis $\hat{H}|\phi_\alpha\rangle = \varepsilon_\alpha|\phi_\alpha\rangle$, we can rewrite Eq. (3) as a system of kinetic equations for $f_{\alpha\beta}(t) = \langle\phi_\alpha|\hat{\rho}(t)|\phi_\beta\rangle$, where we neglect nondiagonal terms if $(\varepsilon_\alpha - \varepsilon_\beta)/\hbar$ are larger than the collision relaxation and generation rates. Thus, for the diagonal terms,

$$\frac{\partial f_{\alpha\alpha}(t)}{\partial t} = G_\alpha(t) + J(f_{\alpha\alpha}|t), \tag{6}$$

where $G_\alpha(t)$ is the photogeneration rate for the α state and $J(f_{\alpha\alpha}|t)$ is the collision integral rate. For the case of ultrafast photoexcitation, using the dipole approximation and the ba-

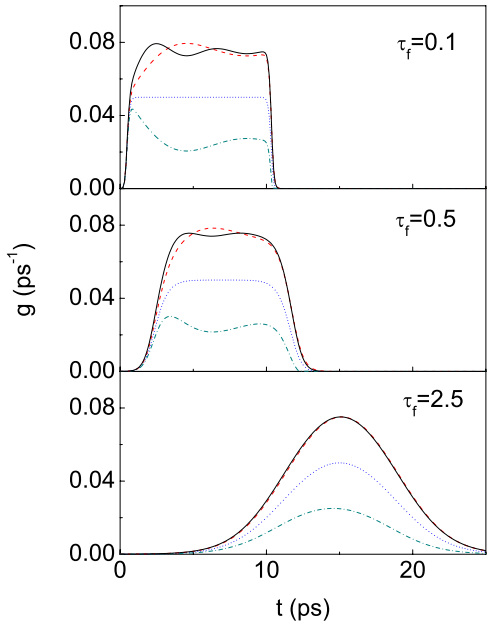

FIG. 3. (Color online) Generation function for $\tau_p=10$ ps and the three τ_f values used in Fig. 2. Solid line: $\Delta=1$ meV. Dashed: $\Delta=0.5$ meV. Dotted: $\Delta=0$ meV. Dash dotted: $\Delta=-0.5$ meV.

sis $|\phi_\alpha\rangle=|n_\alpha\rangle$ with $\alpha=v$ (valence), c (conduction), we get

$$\frac{dn_c(t)}{dt} = G(t) + \left(\frac{\partial n_c}{\partial t}\right)_{sc},$$

$$\frac{dn_v(t)}{dt} = -G(t) + \left(\frac{\partial n_v}{\partial t}\right)_{sc}, \tag{7}$$

where $n_{v,c}(t)$ are the electron densities in the valence and conduction bands. For the case in which there is only photoexcitation, terms $(\frac{\partial n_c}{\partial t})_{sc}=-(\frac{\partial n_v}{\partial t})_{sc}$ correspond to the collision-induced relaxation of population in the conduction and valence bands. If we define the detuning energy as $\Delta=\varepsilon_c-\varepsilon_v-\hbar\omega$, the interband generation rate can be expressed through

$$G(t) = 2\left(\frac{eE_\perp v_{cv}}{\hbar\omega}\right)^2 w(t)\mathrm{Re}\left[\int_{-\infty}^{0} d\tau w(t+\tau)\sin\left(\frac{\Delta\tau}{\hbar}\right)\right], \tag{8}$$

and v_{cv} is the interband velocity. Figure 3 represents the generation function $g(t)=G(t)/N_{\mathrm{ph}}$ for different τ_f and detuning energy values Δ, where

$$N_{\mathrm{ph}} = 2\pi\rho_{2D}[eE_\perp v_{cv}\langle\phi_c(z_e)|\phi_v(z_h)\rangle/\omega]^2\tau_p/\hbar \tag{9}$$

is the characteristic density of photoexcited charges (for $\Delta=0$ meV and $\tau_p=10$ ps; an excitation energy density of 0.2 μJ cm^{-2} corresponds to a characteristic density of 2×10^{10} cm^{-2} in our structure). It is important to point out that the detuning energy only has an appreciable influence in the generation function when $\Delta<1$. Beyond this value, $g(t)$ remains the same for any Δ. Thus, we will use $\Delta=1$ meV from now on. This value is enough to reach the maximum of the generation function.

We will also consider collision-induced relaxation in terms of the generation and annihilation rates. Initially, free electrons are injected quasi-instantaneously or photoexcited and lose their free condition to generate excitons and trions. So we have two annihilation mechanisms expressed through the generation rates Γ_{exc} and Γ_{tr}, respectively. In addition, trion destruction gives rise to free electrons because the recombination of one electron with the hole leaves an additional free electron. The same argument can be used for the positive trion, which gives rise to free holes. Thus, we have an additional generation term for free electrons at a rate $1/\tau_{\mathrm{tr}}$. We define $N_{\mathrm{inj}(e)}$ as the total density of injected electrons and $N_{\mathrm{dif}(h)}$ as the total density of diffused holes. By writing densities of free electrons, holes, excitons, and trions (negative and positive) in units of N_{ph} [$n_e(t)$, $n_h(t)$, $n_{\mathrm{exc}}(t)$, and $n_{\mathrm{tr}(\mp)}(t)$, respectively] and considering that $n_e(t=0)=N_{\mathrm{inj}(e)}/N_{\mathrm{ph}}$ and $n_h(t=0)=N_{\mathrm{dif}(h)}/N_{\mathrm{ph}}$ before switching the pulse on, we get for free electrons

$$\frac{d}{dt}n_e(t) = g(t) + \frac{1}{\tau_{\mathrm{tr}}}n_{\mathrm{tr}(-)}(t) - \Gamma_{\mathrm{tr}}n_e(t)n_h(t)[2n_e(t)+n_h(t)] - \left(\Gamma_{\mathrm{exc}}+\frac{1}{\tau_e}\right)n_h(t)n_e(t) - \Gamma_{\mathrm{tr2}}n_e(t)n_{\mathrm{exc}}(t). \tag{10}$$

Thus, injected electrons and diffused holes are included in the initial boundary conditions. In a similar way excitonic electrons appear—after instantaneous hole diffusion—at a rate Γ_{exc} and disappear due to recombination and trion generation at rates $1/\tau_{\mathrm{exc}}$ and Γ_{tr}, respectively. Thus, for excitonic electrons,

$$\frac{d}{dt}n_{\mathrm{exc}}(t) = \Gamma_{\mathrm{exc}}n_h(t)n_e(t) - \frac{1}{\tau_{\mathrm{exc}}}n_{\mathrm{exc}}(t) - \Gamma_{\mathrm{tr2}}n_{\mathrm{exc}}(t)n[n_e(t)+n_h(t)], \tag{11}$$

and, for negative and positive trion electrons,

$$\frac{d}{dt}n_{\mathrm{tr}(-)}(t) = \Gamma_{\mathrm{tr2}}n_e(t)n_{\mathrm{exc}}(t) + \Gamma_{\mathrm{tr}}n_e^2(t)n_h(t) - \frac{1}{\tau_{tr}}n_{\mathrm{tr}(-)}(t),$$

$$\frac{d}{dt}n_{\mathrm{tr}(+)}(t) = \Gamma_{\mathrm{tr2}}n_{\mathrm{exc}}(t)n_h(t) + \Gamma_{\mathrm{tr}}n_e(t)n_h(t)^2 - \frac{1}{\tau_{\mathrm{tr}}}n_{\mathrm{tr}(+)}(t). \tag{12}$$

Lastly, for the hole density, we can write

$$\frac{d}{dt}n_h(t) = g(t) + \frac{1}{\tau_{tr}}n_{\mathrm{tr}(+)}(t) - \Gamma_{\mathrm{tr}}n_e(t)n_h(t)[n_e(t)-2n_h(t)] - \left(\Gamma_{\mathrm{exc}}+\frac{1}{\tau_e}\right)n_h(t)n_e(t) - \Gamma_{\mathrm{tr2}}n_h(t)n_{\mathrm{exc}}(t). \tag{13}$$

In the absence of photoexcitation, similar expression for double QWs can be found in Ref. 11. In the expressions above, $\Gamma_{\mathrm{tr}}^{-1}$ is the mean time required for trion formation via three-particle processes: two free electrons and a hole for negative trion or two holes and a free electron for positive trion. The intrinsic exciton and trion lifetimes are τ_{exc} and τ_{tr}, respectively, and τ_e is the recombination time of free carriers. Finally, Γ_{tr2} is trion formation rate through two-particle in-

TABLE I. Characteristic generation and relaxation times in ps for low temperature.

τ_e	Γ_{exc}^{-1}	τ_{exc}	Γ_{tr2}^{-1}	Γ_{tr}^{-1}	τ_{tr}
10^4	60	700	710	700	340

teraction: an exciton plus a free electron (hole) for the negative (positive) trion. An extensive analysis of these times can be found in the papers of Esser *et al.*[2] and Deveaud *et al.*[8] Although the majority of coefficients takes into account the mass action law (Saha-Eggert relations), we have considered that the process of exciton formation is much faster than the generation of trions and the annihilation of both excitons and trions.[4] Actually, Γ_{tr2} corresponds to the scattering rate of excitons with free electrons, which give rise to the trion formation. Experimentally, this scattering formation rate is proportional to the free-electron density, to the in-plane exciton area (which contributes to the cross section of the process), and to the kinetic energy of the two interacting species. We have used phenomenological data for 100 Å GaAs-$GaAl_{0.35}As_{0.65}$ QWs included in Refs. 2–4.

III. NUMERICAL RESULTS AND DISCUSSION

To analyze particle densities we numerically perform the coupled system [Eqs. (10)–(13)] using the Runge-Kutta method. We only consider cases in which the density of injected electrons is higher than the density of diffused holes, e.g., an excess of free-electron density of about 10^9–10^{10} cm^{-2}. Higher densities could prevent trion formation.[4] Data used in calculations are included in Table I.

Figures 4(a) and 4(b) represent the density evolution of holes and free exciton and trion electrons $[n_k(t)]$ for the hypothetical initial concentration pair $n_e(0)=0.5$ and $n_h(0)=0.1$. We have used an ultrafast pulse with $\tau_p=10$ ps and $\tau_f=0.1$ ps and a detuning energy $\Delta=1$ meV. Initially, there are only injected free electrons and diffused holes, the density of which increases quickly after switching the pulse on and decays as soon as the pulse is switched off, giving rise to excitons or recombining. These excitons generate trions due to the scattering processes between excitons and free electrons or free holes. Another source of trions are the three-particle processes. The recombination of electron-hole pairs reduces the density of electrons both in excitons and in trions. In the latter case each extinct trion leaves one electron free, which contributes to increasing the stock of remaining free electrons. This recombination leads to a long-time limit of the total density of electrons, which is equal to the free-electron excess, $n_e(t\to\infty)=n_e(0)-n_h(0)$. Figure 4(b) shows the initial stages of the process. The shape of the pulse has little influence on the generation rate when τ_p is shorter than the different characteristic generation and annihilation rates. The fact that the relative concentration of free electrons overcomes the unit in Figs. 4(a) and 4(b) is because densities are normalized to photoexcited characteristic density. The sum of this density, plus that of injected electrons, can be bigger than the unit if characteristic recombination times are long versus the generation rate.

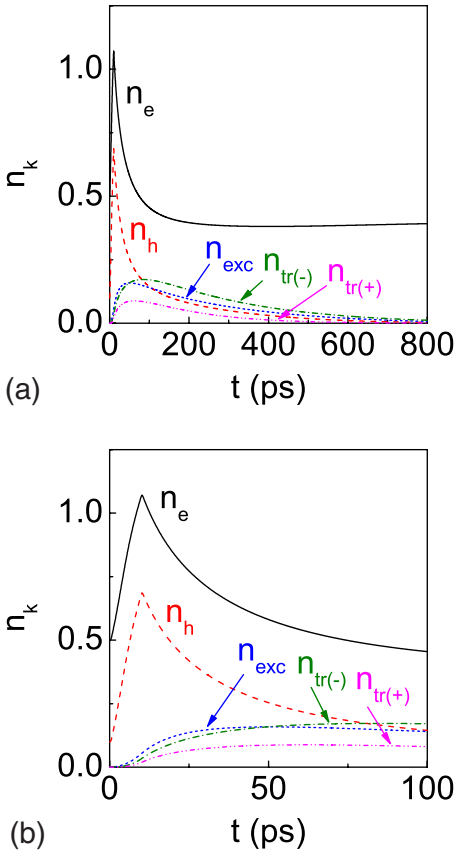

FIG. 4. (Color online) Dimensionless densities for a pulse with $\tau_p=10$ ps and $\tau_f=0.1$ ps. The initial dimensionless doping concentrations are $n_e(0)=0.5$ and $n_h(0)=0.1$. Solid line: free-electron density. Dashed: hole. Dotted: exciton. Dash dotted: negative trion. Dash-dot dotted: positive trion. (b) Corresponds to short-time region.

With the purpose of analyzing the effect of the pulse shape, we have considered a τ_p of the order of the characteristic times of generation and annihilation processes. Figures 5(a)–5(c) show evolution of n_k for pulses of $\tau_p=100$ ps with fronts of $\tau_f=1$, 5, and 25 ps with the same initial concentrations used before. Only in the initial steps of the process, the front pulse has some importance. In this case the negative trion electron density can even exceed the exciton electron density. Due to the large tail of the Gaussian-type pulse [Fig. 5(c)], free-electron and hole densities decay as excitons and trions begin to form, before perceiving photoexcitation pulse.

We now analyze the behavior of $n_k(t)$ as a function of the initial concentrations. To do that, we vary concentrations of donors and acceptors in the doped regions. For a realistic experimental situation of ultrafast photoexcitation, the majority of electrons are photoexcited from the valence band. In such a case, the number of excitons is greater than the number of other complex species as Fig. 6 shows. This situation can be reverted by increasing the doping concentration of donors in the left reservoir beyond $n_e(0)=0.5$ (see Figs. 4 and 5). When $n_e(0)$ and $n_h(0)$ are not very different [Fig. 6(a)], positive and negative trion densities are close to each other and lower than exciton density. Whereas when $n_e(0) \gg n_h(0)$, negative trion density is higher than positive one

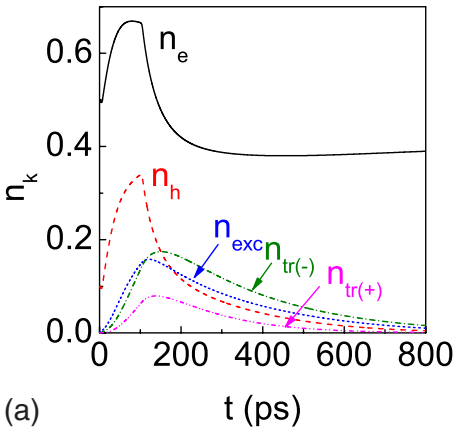

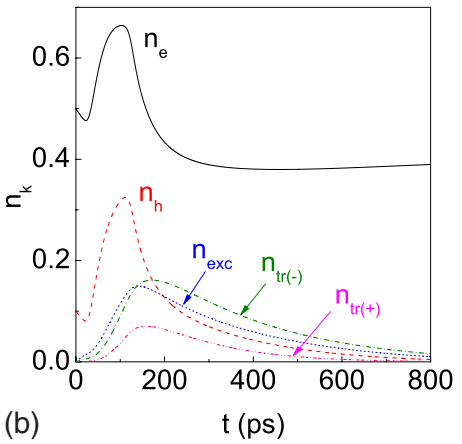

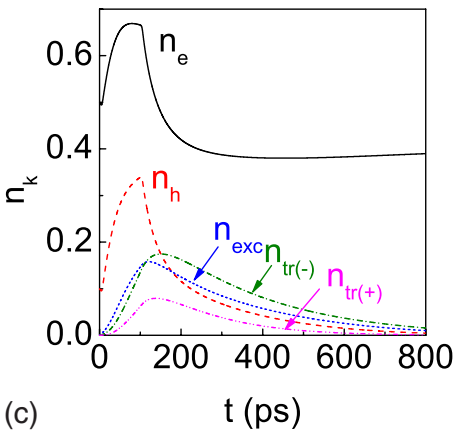

FIG. 5. (Color online) Dimensionless density for long duration pulses with τ_p=100 ps and τ_f=1 ps (a), τ_f=5 ps (b), and τ_f=25 ps (c). Initial densities and lines code are the same as in Fig. 4.

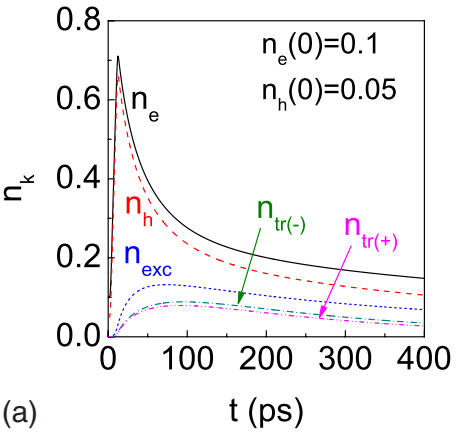

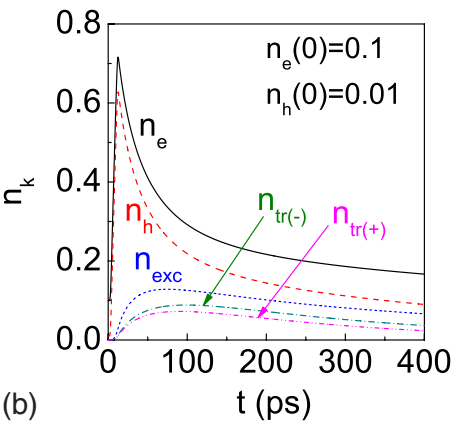

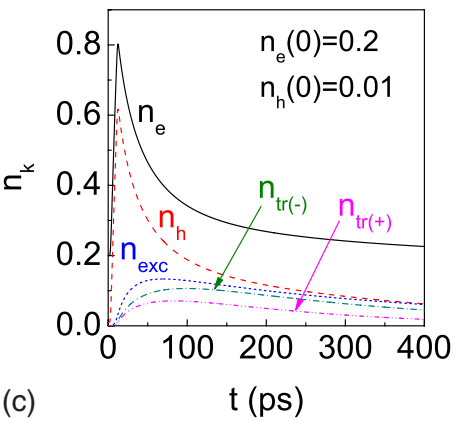

FIG. 6. (Color online) Dimensionless densities for the same pulse of Fig. 4 and for three different initial doping concentrations. Lines code are the same as in former figures.

and comes closer to exciton density [Fig. 6(c)].

It is interesting to check the above results with existing measures. Because PL intensity $I_{\mathrm{PL}}(t) \sim n_k(t)/\tau_k$, where τ_k is the intrinsic lifetime of the species k, density evolution of the excited complexes can be observed by this technique. Figure 7 shows contributions of free-electron (plasma), exciton, and trion densities to the PL intensity $I_{\mathrm{PL}}(t)$ for different pulses and initial concentrations $n_k(0)$. As expected, the duration and shape of the pulses control the behavior of luminescence intensity during a short time. However, temporal tails of luminescence intensity are governed by initial concentrations. Our results for short pulses (τ_p=10 ps) are in reasonable good agreement with the experimental data existing in the literature for GaAs-GaAlAs QWs.[2–5]

For higher densities than those used in the present work, the effect of the electron-electron Coulomb interaction becomes more noticeable due to the space-charge potential energy created by the spatial distribution of electrons and holes. This space-charge potential is repulsive for holes and attractive for electrons. Electron-hole attraction dominates

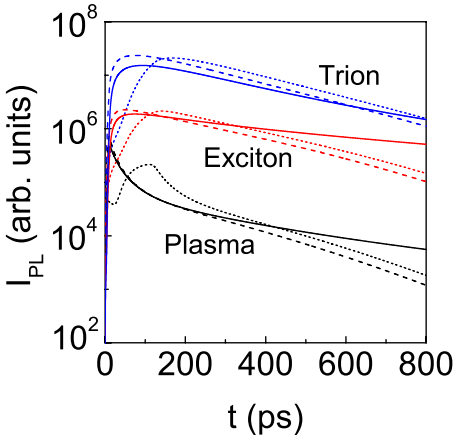

FIG. 7. (Color online) Photoluminescence intensity decay. Solid line: $n_e(0)=0.1$, $n_h(0)=0.05$, and $\tau_p=10$ ps; dashed: $n_e(0)=0.5$, $n_h(0)=0.1$, and $\tau_p=10$ ps; and dotted: $n_e(0)=0.5$, $n_h(0)=0.1$, and $\tau_p=100$ ps.

electron-electron and hole-hole repulsions at low densities. When the carrier density increases the repulsive part of the Hartree-Fock potential energy increases as well. Beyond a certain initial density $[n_e(0) \gtrsim 10^{11}\ \mathrm{cm}^{-2}]$ of free electrons, the repulsion equals the attractive potential. For higher densities, the Coulomb interaction of the second electron with the hole in the trion is canceled resulting in trion extinction, which generates excitons and free electrons. If the free-electron density increases even more, the binding energy of excitons tends to zero and excitons also disappear. These densities mainly affect the dynamics of the level-shift energy of electrons.[11]

The approximations used in the method of calculation should also (now) be mentioned. We assumed that electron injection and hole diffusion are much shorter processes than the pulse duration and the exciton generation time, which, in turn, is even shorter than trion generation and recombination times. Another important point is the possible effect of the applied external electric field on the trions. We have used field intensities, which are lower than 30 kV/cm to prevent the ionization or possible trion diffusion across the structure.[4]

IV. CONCLUSIONS

In summary, we have analyzed the generation of excitons and trions including effects resulting from the interaction of the laser electromagnetic field with photoexcited carriers, an ever-present problem in photoexcitation. We have also included the effect of the shape and duration of the laser pulse. The method is based on electron-tunneling injection and hole diffusion from remotely doped layers[1] together with an ultrafast photoexcitation. We have also analyzed the effect of the coexistence of positive and negative trions together with excitons. We have studied the aforementioned effect using the five-coupled Bloch system obtained from the kinetic equation for the one-electron density matrix and taking into account the five possible time-dependent processes. Our results show a wide variety of responses caused by the different carrier densities of the three systems (electrons, excitons, and trions). Present results can be checked by means of PL measures. PL experiments for trions in single and coupled double QWs are available. We expect that this paper will stimulate experimental studies on the exciton and trion dynamics.

ACKNOWLEDGMENTS

This work has been supported in part by the Ministerio de Educación y Ciencia (Spain) and FEDER under Project No. FIS2005-01672.

*paceituno@yahoo.es

[1] H. Cao, G. Klimovitch, G. Björk, and Y. Yamamoto, Phys. Rev. B **52**, 12184 (1995); Phys. Rev. Lett. **75**, 1146 (1995).
[2] A. Esser, E. Runge, R. Zimmermann, and W. Langbein, Phys. Rev. B **62**, 8232 (2000); Phys. Status Solidi A **178**, 489 (2000).
[3] D. Sanvitto, R. A. Hogg, A. J. Shields, D. M. Whittaker, M. Y. Simmons, D. A. Ritchie, and M. Pepper, Phys. Rev. B **62**, R13294 (2000).
[4] D. Sanvitto, F. Pulizzi, A. J. Shields, P. C. M. Christianen, S. N. Holmes, M. Y. Simmons, D. A. Ritchie, J. C. Maan, and M. Pepper, Science **294**, 837 (2001); F. Pulizzi, D. Sanvitto, P. C. M. Christianen, A. J. Shields, S. N. Holmes, M. Y. Simmons, D. A. Ritchie, M. Pepper, and J. C. Maan, Phys. Rev. B **68**, 205304 (2003).
[5] G. Finkelstein, V. Umansky, I. Bar-Joseph, V. Ciulin, S. Haacke, J.-D. Ganière, and B. Deveaud, Phys. Rev. B **58**, 12637 (1998); D. Sanvitto, R. A. Hogg, A. J. Shields, M. Y. Simmons, D. A. Ritchie, and M. Pepper, Phys. Status Solidi B **227**, 297 (2001).
[6] A. Wójs and J. J. Quinn, Phys. Rev. B **75**, 085318 (2007); A. Wójs, *ibid.* **76**, 085344 (2007); M. Hayne, C. L. Jones, R. Bogaerts, C. Riva, A. Usher, F. M. Peeters, F. Herlach, V. V. Moshchalkov, and M. Henini, *ibid.* **59**, 2927 (1999); A. Wójs, J. J. Quinn, and P. Hawrylak, *ibid.* **62**, 4630 (2000); G. Yusa, H. Shtrikman, and I. Bar-Joseph, Phys. Rev. Lett. **87**, 216402 (2001); C. Schüller, K.-B. Broocks, P. Schröter, Ch. Heyn, D. Heitmann, M. Bichler, W. Wegscheider, T. Chakraborty, and V. M. Apalkov, *ibid.* **91**, 116403 (2003).
[7] F. J. Teran, L. Eaves, L. Mansouri, H. Buhmann, D. K. Maude, M. Potemski, M. Henini, and G. Hill, Phys. Rev. B **71**, 161309(R) (2005).
[8] B. Deveaud, L. Kappei, J. Berney, F. Morier-Genoud, M. T. Portella-Oberli, J. Szczytko, and C. Piermarocchi, Chem. Phys. **318**, 104 (2005); M. T. Portella-Oberli, J. Berney, L. Kappei, F. Morier-Genoud, J. Szczytko, and B. Deveaud, arXiv:0708.2429 (unpublished).
[9] K. Kheng, R. T. Cox, Y. Merle d'Aubigné, F. Bassani, K. Saminadayar, and S. Tatarenko, Phys. Rev. Lett. **71**, 1752 (1993); P. Kossacki, P. Plochocka, B. Piechal, W. Maślana, A. Golnik, J.

Cibert, S. Tatarenko, and J. A. Gaj, Phys. Rev. B **72**, 035340 (2005); I. Camps, S. S. Makler, A. Vercik, Y. Galvão Gobato, G. E. Marques, and M. J. S. P. Brasil, Solid State Commun. **135**, 241 (2005).

[10] S. Ben-Taboude-Leon and B. Laikhtman, Phys. Rev. B **67**, 235315 (2003).

[11] P. Aceituno and A. Hernández-Cabrera, J. Appl. Phys. **98**, 013714 (2005).

[12] F. T. Vasko and O. E. Raichev, *Quantum Kinetic Theory and Applications: Electrons, Photons, Phonons* (Springer, New York, 2005).